Reduction-Based Model Updating of a Scaled Offshore Platform Structure

Hui Li[1] and Hua Ding[2]

Abstract: This paper attempts to develop a reduction-based model updating technique for jacket offshore platform structure. A reduced model is used instead of the direct finite-element model of the real structure in order to circumvent such difficulties as huge degrees of freedom and incomplete experimental data that are usually civil engineers' trouble during the model updating. The whole process consists of three steps: reduction of FE model, the first model updating to minimize the reduction error, and the second model updating to minimize the modeling error of the reduced model and the real structure. According to the performance of jacket platforms, a local-rigidity assumption is employed to obtain the reduced model. The technique is applied in a downscale model of a four-legged offshore platform where its effectiveness is well proven. Furthermore, a comparison between the real structure and its numerical models in the following model validation shows that the updated models have good approximation to the real structure. Besides, some difficulties in the field of model updating are also discussed.

DOI: 10.1061/(ASCE)0733-9399(2010)136:2(131)

CE Database subject headings: Offshore structures; Platforms; Finite element method; Numerical models.

Author keywords: Structural dynamics; Model analysis; Platforms; Scale model.

Introduction

Developing reliable analytical models that can accurately describe or predict the responses of actual structure is very important for load identification problems or coupled-field analysis in structural dynamics. Computer-aided modeling (CAM) and computer-aided test (CAT) are developed to solve this problem but difficulty can exist if either of them is used alone. The CAM, such as finite-element (FE) analysis, now provides a very powerful modeling tool. But FE model may deviate from the real structure because of many artificial simplifications introduced in numerical simulation, which may sometimes be unacceptable. CAT can provide some characteristics of the real structure but it cannot predict the response of the structure under arbitrary excitation. Model updating provides a bridge between CAM and CAT and an efficient way to assure that primitive FE model can be tuned to the actual structure. A remarkable number of methods for FE model updating have been developed in the recent decades, which is discussed in detail by Mottershead and Friswell (1993).

Among the early papers, Berman (1979), Berman and Nagy (1983), Baruch (1984), and Zimmerman and Widengren (1990), the focus was put on direct method, namely, directly adjusting initial mass and stiffness matrices. But this kind of method may change sparse matrices into full ones and causes the updated model to lose the physical connecting properties of its original FE model, i.e., the way that structural design variables are mapped into the elements of structural mass matrices and stiffness matrices. Because of such inherent deficiency, the later studies turned to adjust the structural parameters, e.g., density, modulus, flexural rigidity, and so on. This approach usually keeps the original physical connecting properties of the FE model and is known as indirect updating method or parametric method. Because of this advantage, many parametric methods have been proposed in recent years. Element-by-element sensitivity method was developed by Farhat and Hemez (1993). Inverse eigensensitivity methods have been investigated by Collins et al. (1974) and Lin et al. (1995). Imregun et al. (1995a,b) and Cha and Switkes (2002) presented an updating method using frequency response function (FRF). Modak et al. (2002) compared the updating results using inverse eigensensitivity method and FRF method, respectively, through numerical simulation. Gladwell and Ahmadian (1995) and Ahmadian et al. (1997) studied new parameter selection strategies for model updating. Jaishi and Ren (2005) tried using ambient vibration test results for model updating. Pandey and Barai (1995), Atalla and Inman (1998), Levin and Lievin (1998b), Levin et al. (2000), Lu and Tu (2004), and Chang et al. (2000, 2002) applied artificial neural network to model updating. Levin and Lieven (1998) introduced simulated annealing and genetic algorithms into model updating. During the recent 10 years, a new kind of statistical methodology for model updating and damage detection, which is mainly based on a Bayesian probabilistic theory, has also been developed, such as Katafygiotis and Beck (1998), Beck and Katafygiotis (1998), Katafygiotis and Yuen (2001), Yuen and Katafygiotis (2002), Katafygiotis and Lam (2002), and Lam et al. (2004). This approach has a distinct advantage over the previous methods in that it reasonably considers the uncertainties arising from incomplete measurements, modeling error, and measurement noise.

There is, however, a great difficulty when the FE model updating is applied to complicated dynamic systems with large num-

[1]Associate Professor, The National Astronomical Observatories, Chinese Academy of Sciences, 20A Datun Rd., Chaoyang District, Beijing 100012, China (corresponding author). E-mail: lihui@bao.ac.cn

[2]Professor, Institute of Mechanics, Chinese Academy of Sciences, No. 15 Beisihuanxi Rd., Beijing 100080, China. E-mail: hding@imech.ac.cn

Note. This manuscript was submitted on May 19, 2005; approved on September 4, 2009; published online on January 15, 2010. Discussion period open until July 1, 2010; separate discussions must be submitted for individual papers. This paper is part of the ***Journal of Engineering Mechanics***, Vol. 136, No. 2, February 1, 2010. ©ASCE, ISSN 0733-9399/2010/2-131–142/$25.00.

ber of structural members. The huge mass and stiffness matrices of such structures can make it time-consuming to solve the eigenvalue problem. On the other hand, the limitation of the incomplete measured data becomes more and more serious as the number of degrees of freedom (DOFs) of a dynamic system increases and even causes the updating work to plunge into the trouble of ill-posed problem if the FE model is directly used. Although modal expansion techniques can be taken as a choice to fill up the spatially incomplete modal data, more other problems may arise. Another way is to reduce the huge DOFs of the structure, known as model reduction. This seems more promising because generally only a few of the lowest modes are practically useful for large-scale structures, which means most of the DOFs are redundant.

The generalized model reduction methods can be classified into three groups. The first group is the superposition method of Ritz vectors, such as Wilson et al. (1982), Arnold et al. (1985), and Leger and Wilson (1987), which constructs a group of Ritz vectors and uses them as transformation matrix to reduce the dimension of the model. The second group is what we call slave-DOF-removing methods, in which coordinate transformation is not needed. The oldest and widely used one of such methods may be Guyan reduction (Guyan 1965) but this static reduction method is applicable at a narrow frequency domain near zero. To settle that shortcoming, Kuhar and Stahle (1974) and Paz (1989) proposed dynamic condensation techniques that are valid at a much wider frequency range. O'Callahan (1989) further developed another dynamic reduction method, improved reduced system (IRS), which boosts the accuracy of results and enlarges the valid domain of frequency. Friswell et al. (1995, 1998) developed an iterated IRS and proved its convergence. Other researchers presented similar techniques but with different iterative formulas, such as Suarez and Singh (1992b), Qu and Fu (1998), Kim and Kang (2001), Lin and Xia (2003), and Xia and Lin (2004). Besides, some researchers also attempted to apply this iterative reduction approach to the damped structural systems. Rao (2002) presented an iterative two-sided dynamic condensation technique for unsymmetric structural systems. Qu and Selvam (2005) used an accelerated iterative approach for the viscously damped vibration system. The third group is component modal synthesis methods which are developed from the modal analysis of complicated structure in aerospace engineering. Two core steps of these methods are associated with substructures, namely, the modal analysis and the assembling of the substructures. According to the type of interfaces and substructure assembling, the methods are basically divided as the fixed-interface modal synthesis method (Hurty 1965), the free-interface modal synthesis method (Hou 1969), and the hybrid-interface modal synthesis method (Benfield and Hrude 1971). Later, many researchers improved the three kinds of modal synthesis methods, such as Bampton and Craig (1968), Rubin (1975), Hintz (1975), and Tsuei and Yee (1989). Suarez and Singh (1992b) developed a new method to calculate the lower eigenproperties of a general dynamic system divided into subsystems. Setareh et al. (1992) used the approach to calculate the optimum tuned mass-damper parameters.

As viewed from model updating, there are still many limitations for most of the reduction methods. First, the reduction process is completed by coordinate transformation in most reduction methods. The original physical coordinates may be transformed to a certain kind of modal coordinates which have not obvious physical meanings. Then the difficulty of transformation may exist because the measured spatial data for model updating is based on the physical coordinates. Second, the iterative algorithms, widely used in the second group, may cause the reduced model to lose some or total indispensable connecting properties of its original FE model, which will be unacceptable for the following parameter-based updating work. Finally, for most of the reduction methods, the reduced model will lack self-adjusting ability if the condition in the initial FE modeling changes (e.g., some structural design variables are updated). It is, however, an effective way for model validation after model updating.

Fig. 1. Scaled platform structure

It is difficult to develop a general reduction and updating method for all complicated large-scale structures that can overcome the limitations mentioned above but possible for jacket platform structures. Most of jacket platform structures can be easily divided into two kinds of components: the floors which have most of structural mass and the connectors between two neighboring floors (Figs. 1 and 3). This characteristic makes it convenient to employ substructure-partitioning method for model reduction and obtain a reduced analytical model easily for parametric updating approach. This paper aims to develop a reduction-based parametric updating method for a scaled platform structure which assures that the reduced model is self-adjustable. An emphasis of the work in this paper is put on model reduction because we require that the obtained reduced model should remain the connecting property of the FE model, and the transformed coordinates should still be able to have obvious physical meanings. Moreover, the strategy of model updating is also employed to calibrate the reduced model even during the reduction process.

The following contents of the paper are organized into three sections. The first section discusses the basic theory of a two-step model reduction method. The following section mainly deals with model updating using the obtained reduced model, where a sensitivity-based parametric updating method is employed. Finally in the last section, an experimental application of a scaled model of platform structure is shown to illustrate the effectiveness of the proposed method.

Reduction of FE Model

The proposed method is a two-step procedure. The first step implements the superposition method of Ritz vectors, in which a local-rigidity assumption of floors is introduced to construct the Ritz vectors and transformation matrix. It is different from other

reduction methods in that the reduced model is allowed to have some errors which are produced by the strict assumption. Then the second step is to correct this error by introducing the principle of model updating. It is convenient to keep the connecting property of the reduced model to do so.

Some Preprocesses for FE Model

Because the platform structure has the following characteristics—(1) most of structural mass is on the floors and (2) beam and plate element types are widely used for the FE model—we can take some constraints during the FE modeling. For example, we apply lump mass mode for all elements and ignore the moment inertia of all nodes to greatly reduce DOFs. On the other hand, we partition the whole structure into two types of substructures: modal substructures (horizontal floors and all connecting rods within floors) and the connecting substructures between floors. Then we can redistribute the mass of the connecting substructures into the neighboring floors and apply Guyan reduction method to delete those massless nodes. To do so, we retain the precision of the FE model and make it convenient for the next proposed reduction method.

Construct Ritz Vectors and Obtain the Reduced Model

In the reduction process, the local-rigidity assumption is introduced as follows:

1. Modal substructures are regarded as rigid bodies and their elastic deformation is ignored; and
2. The connecting substructures are still considered flexible.

The above assumptions can be regarded as an approximation of the observations that are found during the modal analysis of the FE model. With above assumptions, a group of Ritz vectors, namely, a transformation matrix, can be constructed so that the complicated FE model is simplified as a spatial cantilever beam (Fig. 3) in which the transformed displacement vectors represent the rigid-body movements of floors. According to the assumptions, the relationship between the rigid-body displacement vector of the ith floor and the displacements of an arbitrary node on it can be expressed as

$$\mathbf{u}_{ij} = \begin{Bmatrix} x_{ij} \\ y_{ij} \\ z_{ij} \end{Bmatrix} = \begin{bmatrix} 1 & 0 & 0 & 0 & 0 & -d_{ij}^{y} \\ 0 & 1 & 0 & 0 & 0 & d_{ij}^{x} \\ 0 & 0 & 1 & d_{ij}^{y} & -d_{ij}^{x} & 0 \end{bmatrix} \begin{Bmatrix} X_i \\ Y_i \\ Z_i \\ \zeta_i \\ \eta_i \\ \theta_i \end{Bmatrix} = \mathbf{\Gamma}_{ij}\boldsymbol{\delta}_i \quad (1)$$

where the x-y plane is assumed parallel to floors; $\mathbf{u}_{ij}$ =displacement vector of the jth node on the ith floor; $\boldsymbol{\delta}_i$=rigid-body displacement vector of the ith floor; $\mathbf{\Gamma}_{ij}$ =transformation matrix of the jth node; and d_{ij}^{x} and d_{ij}^{y} =distances from the jth node to the mass center of the ith floor in the x- and y-directions, respectively. Eq. (1) can be applied to all nodes of the ith floor and even all floors. So we can get

$$\mathbf{u}_i = \begin{Bmatrix} \mathbf{u}_{i1} \\ \vdots \\ \mathbf{u}_{ij} \\ \vdots \\ \mathbf{u}_{il_i} \end{Bmatrix} = \begin{bmatrix} \mathbf{\Gamma}_{i1} \\ \vdots \\ \mathbf{\Gamma}_{ij} \\ \vdots \\ \mathbf{\Gamma}_{il_i} \end{bmatrix} \begin{Bmatrix} X_i \\ Y_i \\ Z_i \\ \zeta_i \\ \eta_i \\ \theta_i \end{Bmatrix} = \mathbf{\Gamma}_i\boldsymbol{\delta}_i \quad (2)$$

$$\mathbf{U} = \begin{Bmatrix} \mathbf{u}_1 \\ \vdots \\ \mathbf{u}_i \\ \vdots \\ \mathbf{u}_r \end{Bmatrix} = \begin{bmatrix} \mathbf{\Gamma}_1 & & & & \\ & \ddots & & & \\ & & \mathbf{\Gamma}_i & & \\ & & & \ddots & \\ & & & & \mathbf{\Gamma}_r \end{bmatrix} \begin{Bmatrix} \boldsymbol{\delta}_1 \\ \vdots \\ \boldsymbol{\delta}_i \\ \vdots \\ \boldsymbol{\delta}_r \end{Bmatrix} = \mathbf{\Gamma}\boldsymbol{\Delta} \quad (3)$$

where the subscript "r"=number of floors; the subscript l_i =number of nodes in the ith floor; $\mathbf{U}=3n\times 1$ (n is the number of nodes) displacement vector of the FE model; $\boldsymbol{\Delta}=6r\times 1$ rigid-body displacement vector of all floors; and $\mathbf{\Gamma}=3n\times 6r$ transformation matrix for the whole FE model. Using $\mathbf{\Gamma}$, we can obtain the reduced stiffness and mass matrices

$$\begin{cases} \mathbf{K}_R = \mathbf{\Gamma}^{\mathrm{T}}\mathbf{K}\mathbf{\Gamma} \\ \mathbf{M}_R = \mathbf{\Gamma}^{\mathrm{T}}\mathbf{M}\mathbf{\Gamma} \end{cases} \quad (4)$$

where $\mathbf{K}$ and $\mathbf{M}$=stiffness and mass matrices of the FE model, respectively, and the subscript R refers to the reduction. Because the order of the reduced model is different from the FE model, it is difficult to calculate the modal assurance criteria (MAC) when directly using the ith mode shape of the FE model: $\boldsymbol{\varphi}_i$. So we introduce the equivalent reduced mode shapes of the FE model which have the same order of the reduced model. Using Eq. (3) and replacing U, Δ with $\boldsymbol{\varphi}_i$ and $\boldsymbol{\varphi}_i^{\mathrm{E}}$, respectively, then multiplying two sides of the equation with the pseudoinverse of $\mathbf{\Gamma}$, we can get

$$\boldsymbol{\varphi}_i^{\mathrm{E}} = (\mathbf{\Gamma}^{\mathrm{T}}\mathbf{\Gamma})^{-1}\mathbf{\Gamma}^{\mathrm{T}}\boldsymbol{\varphi}_i \quad (5)$$

where $\boldsymbol{\varphi}_i^{\mathrm{E}}$=$i$th equivalent mode shapes.

Eq. (4) makes it possible to reduce the thousands of DOFs of the FE model to only a few rigid-body DOFs of floors. It not only spares computation time and resources in structural eigenproblem analysis but also provides an optimized design plan for modal experiment. Moreover, the parametric updating method can be used for the reduced model because the original connecting property of the FE model is remained during the reduction processes since the original stiffness and mass matrices appear in the right side of Eq. (4).

First Model Updating—Eliminate the Error Caused by Reduction

The local-rigidity assumption makes the reduction process quite simple and convenient but it also brings error. The error is admissible because the elastic deformation within floors caused by structural vibration cannot be completely ignored. Otherwise, it means the stiffness of floors is infinite or additional constrain must be applied to floors, both of which actually overvalue the stiffness of the structure. As a result, the natural frequencies of the reduced model always increase, which means that the reduced model cannot be taken as an effective equivalence of the FE model, not to mention applying it for experiment-based model updating. On the other hand, the error should be in, somehow, control. For example, it is no larger than FE-test discrepancy or has at most the same level. Otherwise, it shows that the local-rigidity assumption does not have a good approximation and the reduction method cannot be applied here. The error should be minimized before the reduced model can be used. However, because of its high efficiency in reduction, the local-rigidity assumption is not selected to be updated in the following procedure of correcting error. Then we should find another equivalent way.

Select Updating Parameters—Submatrix Scaling Factors

According to the aforementioned analysis, the error is mainly caused by the overvaluation of stiffness of floors. Therefore, the stiffness matrix of the reduced model will be updated to eliminate such an error but the mass matrix will keep unchanged. A submatrix scaling technique used by Lim (1990) and Yun and Bahng (2000) is applied in correcting error to avoid changing the local-rigidity assumptions. Since the assumption is implemented by introducing matrix $\mathbf{\Gamma}$, and submatrix $\mathbf{\Gamma}_i$ constrains the node displacements of the ith floor, we can use $\alpha_i\mathbf{\Gamma}_i$ to replace $\mathbf{\Gamma}_i$ as a way to reevaluate the validity of the constraint. Here α_i is a positive number less than 1. We call α_i as the submatrix scaling factor (SSF) of the ith floor. When α_i converges to 1, it implies the local-rigidity assumption approaches to the reality for the ith floor. So the transformation matrix $\mathbf{\Gamma}$ can be modified as

$$\mathbf{\Gamma}_U = \sum_{i=1}^{r} \alpha_i \boldsymbol{\gamma}_i = \sum_{i=1}^{r} \alpha_i \begin{bmatrix} 0 & & & & \\ & \ddots & & & \\ & & \mathbf{\Gamma}_i & & \\ & & & 0 & \\ & & & & \ddots \end{bmatrix} \tag{6}$$

where the subscript "U" means "updated." Then the modified reduced stiffness matrix $\mathbf{K}_R$ can be rewritten as

$$\mathbf{K}_R = \mathbf{\Gamma}_U^{\mathrm{T}}\mathbf{K}\mathbf{\Gamma}_U = \sum_{i=1}^{r}\sum_{j=1}^{r}(\alpha_i\alpha_j)(\boldsymbol{\gamma}_i^{\mathrm{T}}\mathbf{K}\boldsymbol{\gamma}_j) = \sum_{i=1}^{q}\sum_{j=1}^{q}\tilde{\alpha}_{ij}\tilde{\mathbf{K}}_{ij} \tag{7}$$

where $\tilde{\mathbf{K}}_{ij}$ represents a force tensor imposed on the ith floor for a unit displacement tensor given on the jth floor and $\tilde{\alpha}_{ij}$ suggests what degree of approximation $\tilde{\mathbf{K}}_{ij}$ is from the real value. Therefore the stiffness matrix will be updated by adjusting the value of α_i while removing the disadvantage caused by introducing the assumptions. As for the reduced mass matrix, Eq. (4) will still be used.

Construct Error Function

The error caused by the assumption may be expressed using different data and in different ways. In our research, the error is composed of two parts. One is natural frequency error between the reduced model and the FE model, expressed as E_ω; the other is mode shape error between two models, expressed as E_ϕ. Both of the errors are constructed based on least-square (LS) principle. Their dimensionless forms are expressed as

$$E_{\omega i} = \frac{\omega_i^{\mathrm{R}} - \omega_i}{\omega_i} \quad \text{and} \quad E_{\phi i} = \frac{1 - \mathrm{MAC}(\boldsymbol{\varphi}_i^{\mathrm{E}}, \boldsymbol{\varphi}_i^{\mathrm{R}})}{\mathrm{MAC}(\boldsymbol{\varphi}_i^{\mathrm{E}}, \boldsymbol{\varphi}_i^{\mathrm{R}})} \tag{8a}$$

where ω_i and ω_i^{R}=ith natural frequency of the FE model and reduced model, respectively. MAC$(\cdot)$ in Eq. (8a) is a function calculating the MAC value, expressed by

$$\mathrm{MAC}(\boldsymbol{\varphi}_i^{\mathrm{E}}, \boldsymbol{\varphi}_i^{\mathrm{R}}) = \frac{[(\boldsymbol{\varphi}_i^{\mathrm{E}})^{\mathrm{T}}\boldsymbol{\varphi}_i^{\mathrm{R}}]^2}{[(\boldsymbol{\varphi}_i^{\mathrm{E}})^{\mathrm{T}}\boldsymbol{\varphi}_i^{\mathrm{E}}][(\boldsymbol{\varphi}_i^{\mathrm{R}})^{\mathrm{T}}\boldsymbol{\varphi}_i^{\mathrm{R}}]} \tag{8b}$$

Therefore, we obtain the error function as

$$J_1 = \frac{1}{2}\sum_{i=1} W_{\omega i}(E_{\omega i})^2 + \frac{1}{2}\sum_{i=1} W_{\phi i}(E_{\phi i})^2 = E_\omega + E_\phi \tag{9}$$

where $W_{\omega i}$ and $W_{\phi i}$=ith weighting coefficients of frequency error and MAC error, respectively, and represent the reliability for each selected mode. Thus an unconstrained optimization problem, i.e., the work of first mode updating, is set up in which the error between the FE and reduced model can be minimized by adjusting $\alpha_i (i=1,\ldots,r)$.

Optimization Algorithm

In our research, the Gauss-Newton method, one of standard LSs optimization algorithm, is adopted to minimize the error expressed by Eq. (9). The partial derivatives of the error function with respect to α_j can be expressed as

$$\frac{\partial J_1}{\partial \alpha_j} = \sum_{i=1} W_{\omega i}E_{\omega i}\frac{\partial E_{\omega i}}{\partial \alpha_j} + \sum_{i=1} W_{\phi i}E_{\phi i}\frac{\partial E_{\phi i}}{\partial \alpha_j} \quad (j=1,2,\ldots) \tag{10a}$$

where

$$\frac{\partial E_{\omega i}}{\partial \alpha_j} = \frac{1}{\omega_i}\frac{\partial \omega_i^{\mathrm{R}}}{\partial \alpha_j} \tag{10b}$$

$$\frac{\partial E_{\phi i}}{\partial \alpha_j} = \frac{1}{\mathrm{MAC}(\boldsymbol{\varphi}_i^{\mathrm{R}}, \boldsymbol{\varphi}_i^{\mathrm{R}})}\left[\frac{(\boldsymbol{\varphi}_i^{\mathrm{R}})^{\mathrm{T}}\dfrac{\partial \boldsymbol{\varphi}_i^{\mathrm{R}}}{\partial \alpha_j}}{(\boldsymbol{\varphi}_i^{\mathrm{R}})^{\mathrm{T}}\boldsymbol{\varphi}_i^{\mathrm{R}}} - \frac{(\boldsymbol{\varphi}_i^{\mathrm{E}})^{\mathrm{T}}\dfrac{\partial \boldsymbol{\varphi}_i^{\mathrm{R}}}{\partial \alpha_j}}{(\boldsymbol{\varphi}_i^{\mathrm{E}})^{\mathrm{T}}\boldsymbol{\varphi}_i^{\mathrm{R}}}\right] \tag{10c}$$

Here, the calculation of $\partial\omega_i^{\mathrm{R}}/\partial\alpha_j$ and $\partial\boldsymbol{\varphi}_i^{\mathrm{R}}/\partial\alpha_j$ are presented with Eqs. (18) and (19) in Appendix I. Using Eq. (10a), the gradient vector and the Hessian matrix of error function, including the search direction, can be easily obtained. To improve the iteration efficiency, the magnitude of the direction vector is controlled to assure descent of error.

Model Updating (Experiment-Based)

The work of first model updating only resolves the problem whether or not the reduced model can have the same performance as the original FE model. Therefore, the reduced model has to be further updated according to the experimental data so that it can accurately describe or predict the responses of actual structures as the measured data show. Furthermore, the second updating process is to minimize the error between the reduced model and the actual structure.

Error Function

Many types of experimental data can be used to build the error function in the second model updating, such as natural frequency, mode shape, antiresonance frequency, all kinds of response spectrum, FRF, and so on. We used natural frequencies and mode shapes for the updating because they can be easily obtained from experiments and are also suitable for the sensitivity analysis. Similar to the first model updating, the error function here adopts the form of Eq. (9) but ω_i and φ^{E} are changed to the measured frequency ω_i^{M} and mode shape $\boldsymbol{\varphi}_i^{\mathrm{M}}$, respectively. Because the mode shapes directly measured are incomplete, $\boldsymbol{\varphi}_i^{\mathrm{M}}$ are obtained through a transformation different from Eq. (4), which is presented in Appendix II. Thus the error function is expressed as

$$\begin{cases} J_2 = \bar{E}_\omega + \bar{E}_\phi = \dfrac{1}{2}\displaystyle\sum_{i=1}^{q} N_{\omega i}(\bar{E}_{\omega i})^2 + \dfrac{1}{2}\sum_{i=1}^{q} N_{\phi i}(\bar{E}_{\phi i})^2 \\ \bar{E}_{\omega i} = \dfrac{\omega_i^{\mathrm{R}} - \omega_i^{\mathrm{M}}}{\omega_i^{\mathrm{M}}}, \quad \bar{E}_{\phi i} = \dfrac{1 - \mathrm{MAC}(\boldsymbol{\varphi}_i^{\mathrm{M}}, \boldsymbol{\varphi}_i^{\mathrm{R}})}{\mathrm{MAC}(\boldsymbol{\varphi}_i^{\mathrm{M}}, \boldsymbol{\varphi}_i^{\mathrm{R}})} \end{cases} \tag{11}$$

where q=number of experimental modes that are used and $\bar{E}_{\omega ii}$ and $\bar{E}_{\phi ii}$=ith experiment-based frequency error and MAC error, respectively. $N_{\omega i}$ and $N_{\phi i}$ are the ith corresponding weighting coefficients for $\bar{E}_{\omega i}$ and $\bar{E}_{\phi i}$, respectively.

Select Updating Parameters and Optimization Algorithm

Compared with constructing error function, selecting suitable structural updating parameters is more difficult and maybe the most challenging work in the field of model updating. Erroneous modeling, FE discretization, uncertain value of structural parameters, and noise-polluted measured data can invariably cause errors. A selection strategy suggests how one thinks modeling error happens and where it comes from. Moreover, different selection strategies may cause quite different updated results. On many occasions, erroneous modeling is the main contributor of the error in the case of industrial and civil buildings, such as uncertain boundary conditions and inaccurate modeling structural joints, which have plagued designers and engineers for many years. On such conditions, ideal assumptions must be abandoned and certain equivalent structural parameters should be introduced to simulate the actual structure during FE modeling. Generally speaking, it is not practical to consider all types of errors compared with limited experimental data. One preferable way is to set up a threshold to single out a few largest errors and then select updating parameters according to the selected errors. This method, also called error-locating method, seeks the largest errors by comparing the difference for each element between the energy obtained from computation and that from experimental results. However, the incomplete experimental data may make the computation of energy difficult. As an alternative, the sensitivities of error function with respect to the different structural parameters can be easily calculated and compared with each other. Similar to error-locating method, the maximum-sensitivity-based method is applied in our research. All possible parameters are taken into account and their respective sensitivities are calculated but a threshold will be set up for comparison and only a small part of them having the largest sensitivities will be singled out and adjusted during each updating pace. The method not only satisfies the principle of the minimum perturbation of parameters but makes the optimization problem determinate at the same time. Based on this strategy, the standard conjugate gradient method can be used to find a minimum of the error function that has physical meanings.

Similar to Eq. (11), the derivative of the error function with respect to structural updating parameters can be expressed as

$$\frac{\partial J_2}{\partial p_j} = \sum_{i=1}^{q} N_{\omega i}\bar{E}_{\omega i}\frac{\partial \bar{E}_{\omega i}}{\partial p_j} + \sum_{i=1}^{q} N_{\phi i}E_{\phi i}\frac{\partial \bar{E}_{\phi i}}{\partial p_j} \tag{12a}$$

where

$$\frac{\partial \bar{E}_{\omega i}}{\partial p_j} = \frac{1}{\omega_i^{\mathrm{M}}}\frac{\partial \omega_i^{\mathrm{R}}}{\partial p_j} \tag{12b}$$

$$\frac{\partial \bar{E}_{\phi i}}{\partial p_j} = \frac{1}{\mathrm{MAC}(\boldsymbol{\varphi}_i^{\mathrm{M}}, \boldsymbol{\varphi}_i^{\mathrm{R}})}\left[\frac{(\boldsymbol{\varphi}_i^{\mathrm{R}})^{\mathrm{T}}\dfrac{\partial \boldsymbol{\varphi}_i^{\mathrm{R}}}{\partial p_j}}{(\boldsymbol{\varphi}_i^{\mathrm{R}})^{\mathrm{T}}\boldsymbol{\varphi}_i^{\mathrm{R}}} - \frac{(\boldsymbol{\varphi}_i^{\mathrm{M}})^{\mathrm{T}}\dfrac{\partial \boldsymbol{\varphi}_i^{\mathrm{R}}}{\partial p_j}}{(\boldsymbol{\varphi}_i^{\mathrm{M}})^{\mathrm{T}}\boldsymbol{\varphi}_i^{\mathrm{R}}}\right] \tag{12c}$$

where p_j=jth structural updating parameter. The calculation of structural eigensensitivity with respect to $p_j (j=1,\ldots,m)$ is given in Appendix I. Then Eq. (12a) can be used to obtain the gradient of error function and the search direction. Similarly, the magnitude of the direction vector is controlled to assure descent of error for each search pace.

Experimental Application

Main Feature of the Structure

An experimental example of a scaled structure of shear-type jacket offshore platform (Figs. 1 and 3) is given to illustrate the implementation of the aforementioned method. The structure is 1.92 m high and 1.04 m wide at the bottom, mainly made of steel, and fixed to the ground through its four legs. It is a three-dimensional (3D) beam-plate composite structure with four steel-reinforced rubber vibration isolators placed between two steel plates and is partitioned into five main structural parts. Some of its initial structural design variables are listed in Table 1.

Computer-Aided Test

We carried out modal test analysis for the scaled structure. The structure was excited by an automatic closed loop control-feedback system and the input force is controlled by a sinusoidal frequency-scanning signal. The frequency of signal is linearly added from 3 to 30 Hz in about 7 min so that stable responses can be obtained for every frequency point. Meanwhile, the amplitude of signal is designed to remain constant. The acceleration FRFs are automatically measured by the loop control-feedback system based on the following equation:

$$H_{ij}(\omega) = \frac{a_i(\omega)}{F_j(\omega)} \tag{13}$$

where $a_i(\omega)$=Fourier transformation of the acceleration response signal in the time domain, measured from the ith DOF and $F_i(\omega)$=Fourier transformation of the excitation force signal applied at the jth DOF. The small dots and arrows in Fig. 3 show the positions of the accelerometers and their measuring directions. Fig. 2 gives three examples of measured acceleration FRFs. Then the modal data of the structure, such as the first five natural frequencies, the corresponding modal damping ratios, and mode shapes of the structure were identified from the experimental data. Fig. 4 shows the five experimental natural frequencies and mode shape values on the selected subsets of DOFs, where five corresponding analytical modal parameters (reduced model) are also given for comparison. Here the experimental mode shapes could not be directly used for the reduced model before they were transformed but Eq. (5) could not be used either because the experimental mode shapes are usually incomplete for the FE model. According to the displacement relationship given by the local-rigidity assumption, we took another way to obtain equivalent experimental mode shapes for the reduced model, as shown in Appendix II. The identified natural frequencies and equivalent mode shapes would be used for the following work of model updating. Because the measured modal damping ratios are small

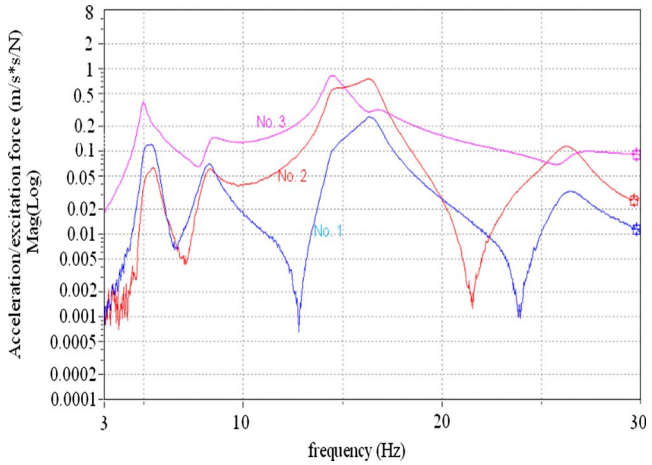

Fig. 2. Acceleration FRFs obtained from three measuring points

(<0.04), it is reasonable and convenient to ignore the damping ratios during the model reduction and updating processes and then introduce them into the updated reduced model for dynamic analysis.

Finite-Element Modeling and Model Reduction (the First Step)

The FE modeling plan was finished in ANSYS software package, in which every line segment of the solid model was meshed as a single beam element (ANSYS modeling and meshing guide—ANSYS release 7.1, May 2003; ANSYS Incorporated, unpublished internal materials). The whole structure was discretized as 493 elements and 486 nodes. All elements were classified into three types, i.e., 3D beam element for Part 1 and Part 5, shell element for Part 2 and Part 3, and linear spring element for Part 4, as shown in Table 1. Lump mass was used for all elements except for the horizontal connectors and bracings between upper deck and down deck which was regarded as massless because of small

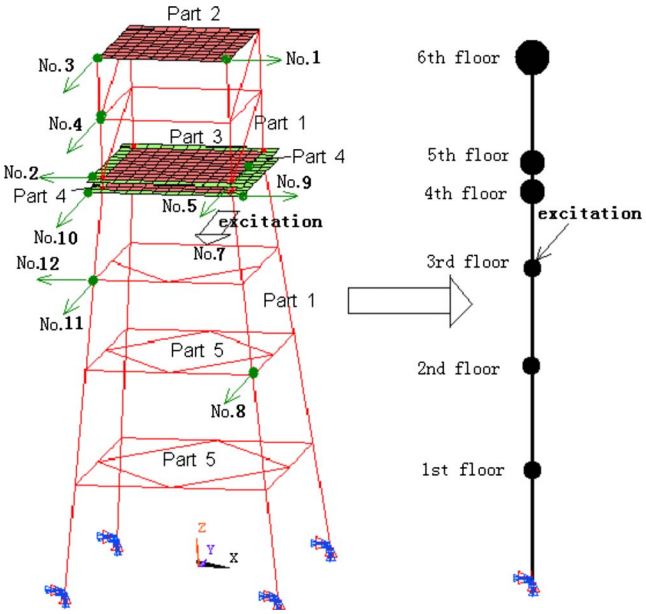

Fig. 3. Distribution of accelerometers and the reduction of model (3D cantilever beam)

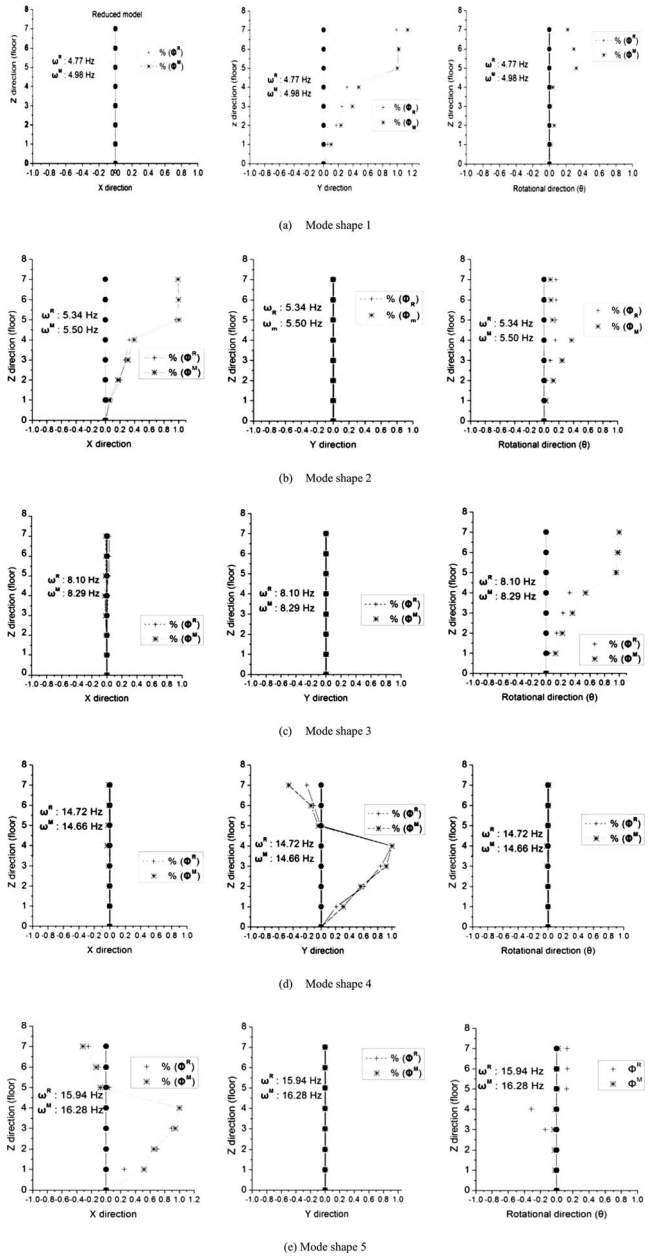

Fig. 4. Analytical and measured modal parameters for the reduced model superscript "*M*": measured; *R*: analytical

dimensions so the total structural mass was distributed to the six floors. We used Guyan method to delete these massless nodes and obtained the final FE model.

During the following model reduction, the local-rigidity assumption was applied to the six floors and the structure was simplified as a 3D cantilever beam, as shown in Fig. 3. Thus the number of the total DOFs was reduced to only 36, namely, six rigid-body DOFs for each floor. Then we got the 36×36 mass and stiffness matrices at the first step of the reduction process. In Table 2, we list the first five natural frequencies of the FE model, reduced model, and test, respectively, and compare three kinds of modal discrepancies: reduced FE, reduced test, and FE test. The table shows relatively high reduced-FE MAC value and obviously higher natural frequencies of the reduced model. The former indicates a better correlation between the FE and reduced models. It can be found that reduced-test modal error and reduced-FE modal

error are obviously larger than FE-test modal error, especially for the fourth and fifth modes. We can make certain that it is mainly caused by the error introduced during the reduction process because the former two modal errors of the fourth and fifth modes are nearly the same. Moreover, the reduced-test and FE-test MAC values are also quite similar to each other. The local-rigidity assumption makes the reduced model overstiff and its natural frequencies higher than those of FE model. However, this effect is not so obvious for the first three modes, where there is no large discrepancy for these modal errors. The facts imply that there is still something reasonable to apply the local-rigidity assumption in the reduction of the structure. Since the reduction error is the main cause, the first updating process is then needed to eliminate it so that the modal errors can decrease and the reduced model can be used.

Model Reduction (the Second Step)—Updating

We selected the first six modes, which is enough for the dynamic analysis of the platform structure, as the object of correcting the error of the reduced model. However, we have to admit that it is quite difficult for the assignment of the weighting factors. There is more art than science to do it. On many occasions, it depends on a balance between the measurement accuracy and the engineer's experience and priority knowledge. The general principle is that the former is more important than the latter and the lower mode is more important than the higher one because of the incompleteness of the measured mode shapes and the fact that experimental natural frequencies have higher precision than mode shapes. However, the condition is a little different in the paper. In Eq. (8*a*), the denominator ω_i in the frequency error $E_{\omega i}$ is increasing with the subscript "*i*." It means that for the same absolute frequency error, the dimensionless $E_{\omega i}$ will not give the same changing rate for the different subscript *i*. Let us consider rewriting Eq. (12*a*) as follows:

$$J_1 = \frac{1}{2}\sum_{i=1} \hat{W}_{\omega i}(\hat{E}_{\omega i})^2 + \frac{1}{2}\sum_{i=1} W_{\phi i}(E_{\phi i})^2 \tag{14}$$

where $\hat{W}_{\omega i}=(\omega_1/\omega_i)^2 W_{\omega i}$ and $\hat{E}_{\omega i}=\omega_i^{\mathrm{R}}-\omega_i/\omega_1$. Then the aforementioned principle can be applied under this new expression form so we take the weight vectors as follows:

$$\{W_\omega\}=\{(\omega_1)^2,\ (\omega_2)^2,\ 0.64(\omega_3)^2,\ 0.64(\omega_4)^2,\ 0.25(\omega_5)^2,\ 0.01(\omega_6)^2\}=\{22.70,\ 28.569,\ 643.894,\ 137.969,\ 64.617,\ 5.265\}$$

$$\{W_\phi\}=\{1,\ 1,\ 1,\ 1,\ 1,\ 1\} \tag{15a}$$

where $\omega_i(i=1,2,\ldots,6)$=natural frequencies of the FE model. It is equivalent that

$$\{\hat{W}_\omega\}=\{1,\ 1,\ 0.64,\ 0.64,\ 0.25,\ 0.01\} \tag{15b}$$

Besides, we also consider that an equal weighting factor of 22.7 for all frequency errors is used for updating. The result shows that the finally updated natural frequencies do not change very much but a better accuracy of the first four updated natural frequencies is observed in the weighting factors in Eq. (15*a*) so we prefer to use Eq. (15*a*) in the paper. Accordingly, six relevant SSFs, corresponding to six floors, were selected as the parameters for the first updating process and their initial values were set to 1.0. Then an optimization problem was built. We solved this problem using Gauss-Newton iterative algorithm. Eqs. (18) and (19) were used to calculate the eigensensitivities with respect to the SSFs and the gradient of the error function.

Updating Results

Fig. 5 shows the procedure diagram of the first model updating, where ε was set to be equal to 0.001 as the criterion for convergence. The optimization iteration was carried out for 12 paces when the criterion was satisfied. Fig. 6 shows that the six SSFs decrease to 1 after the iteration, which means the assumption in the reduction process gives an overvaluation of the actual stiffness of each floor. On the other hand, the fact that most of the updated SSFs are larger than 0.9 indicates the reasonability of the assumption. Fig. 7 compares the relative natural frequency error of the reduced model, where a great decrease can be observed for all six modes after the first updating. Fig. 8 shows the change of six reduced-FE MAC values. There are some improvements for the MAC values but not so obvious as for the frequency errors because the initial MAC values are near to 1, thus the mode shape contribution for the total error is small.

Second Model Updating (Experiment-Based)

Error Function

The first five measured natural frequencies and equivalent mode shapes on the selected subsets of DOFs were used to build the

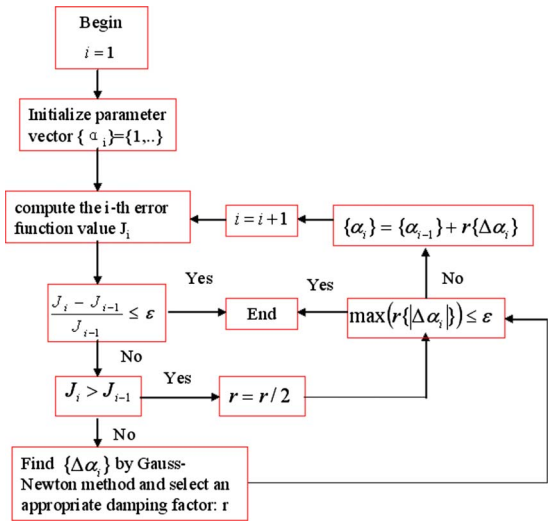

Fig. 5. Procedure of the first model updating

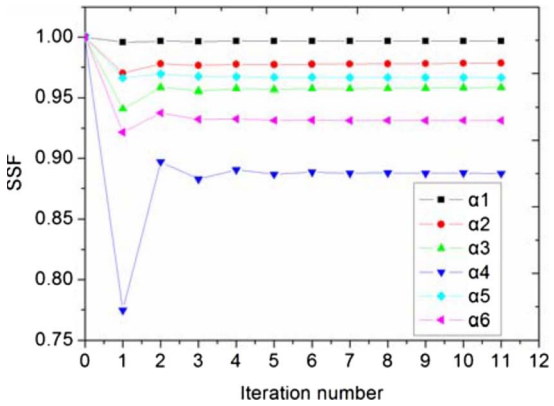

Fig. 6. Change of SSFs (first updating)

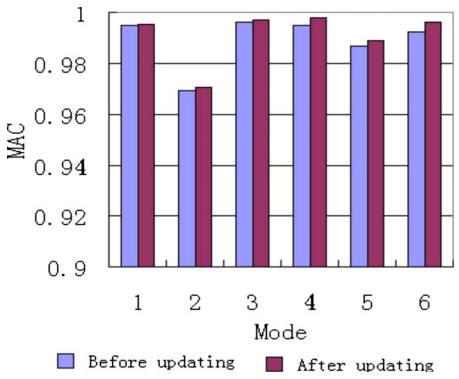

Fig. 8. Change of reduced-FE MAC (first updating)

error function for the second model updating. Generally, there is more art than science on how to select weights. Similar to the first updating, the final updating results are not very sensitive to the obvious change of weights. But this also means that there may be quite a few suitable selections for an arbitrary accuracy. Then a so-called optimized selection depends on a balance between the measurement accuracy and the engineer's experience and priority knowledge. Here our strategy is to consider the measurement accuracy and make the total final frequency errors minimized. The values of the weighting factors mainly depend on the precision of the different experimental data. In the paper, the weight vectors were finally taken as follows:

$$\{N_\omega\} = \{200,\ 200,\ 200,\ 200,\ 200\}$$

$$\{N_\phi\} = \{4,\ 1,\ 1,\ 4,\ 1\} \tag{16}$$

Here we set the same weights for all frequency errors and they are much higher compared with the MAC errors because all the measured natural frequencies have the similar precision and are much more creditable than the measured mode shapes. Besides, the first and fourth mode shapes are more creditable than others because the excitation direction is consistent with their main vibration directions so their weighting factors were taken higher.

Select Parameters for Updating

Theoretically, all possible structural variables can be selected for adjustment in the updating. It is however computationally costly, even impossible, if too many variables are included. To limit the number of the unknown variables to an acceptable level, the parameters are taken for updating with the following strategies. First, all the material variables, e.g., density and modulus, do not vary for the same structural part or the same element type. Second, some larger geometrical dimensions of the structure, such as length and width, are not included since they are easy to measure under the well-controlled experimental conditions. Last, because the boundary and connection conditions can be simulated with reasonable confidence in the laboratory environment, they are also not chosen. Then, a total of nine parameters were selected for updating, as shown in Table 3. To make the comparison among different parameters convenient, we used dimensionless relative difference to trace the change of these nine parameters in the updating process. For the parameter p, the relative difference is expressed as

$$\Delta p = \frac{p_u - p_{\text{ref}}}{p_{\text{ref}}} \times 100\% \tag{17}$$

where p_u and p_{ref}=updated value and the original reference value of p, respectively.

The conjugate gradient method was employed to solve this optimization problem. Eqs. (20) and (21) were used to calculate the eigensensitivities with respect to the structural parameters and the gradient of the error function. For each iteration pace, four largest of the total nine derivatives were singled out and then their corresponding parameters were adjusted. The basic principle of the whole optimization procedure is similar to Fig. 4.

Updating Results

In updating process, the error function descended and converged to a minimum essentially after 15 iterations. Fig. 9 shows the

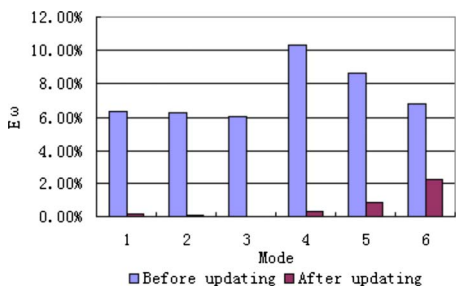

Fig. 7. Change of relative frequency error (first updating)

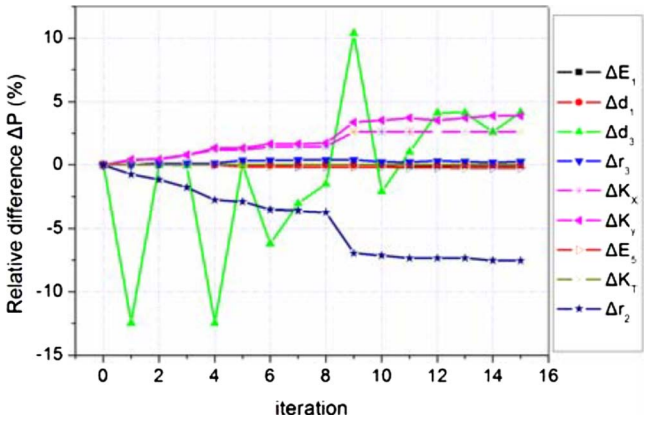

Fig. 9. Change of structural parameters (second updating)

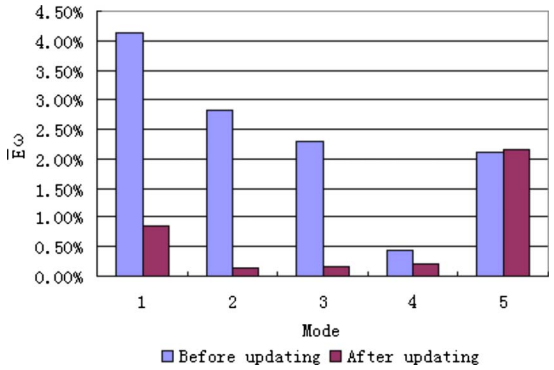

Fig. 10. Change of reduced-test frequency error (second updating)

changes of the nine parameters. It can be observed that there is an obvious and smooth change that happened on the translational spring stiffness K_x, K_y, and the mass density ρ_2. On the other hand, the parameter d_1 shows a great but abrupt fluctuation at the beginning but it gradually settles at a lower level. The improvements of the four parameters mainly contribute to the decrease of the total error so we consider them as the main cause of modeling error. Figs. 10 and 11 show the improvements of relative frequency errors and MAC values after the updating. There are obvious improvements for the first four modes in Fig. 10, except for the fifth mode which even becomes a little worse. The facts suggest that there are still some discrepancies between the analytical model and real structure. One possible explanation is that the way that the rubber isolator is simplified as linear spring in the FE modeling may not be good for the higher mode.

Validation of the Reduced Model

Once the updating is finished, we obtained an updated reduced model and a group of updated structural parameters. Using these updated parameters for FE remodeling, we can get an updated FE model. If the proposed method is reasonable, the updated FE model and the updated reduced model should still have good consistency with each other. Therefore, we made a comparison in Table 4 for these two models. The table lists the first five natural frequencies and MAC value before and after the second updating, respectively. It can be seen from the table that the new MAC value change very little relative to the old. A good consistence of the first four natural frequencies still exists for the two updated models and they have a better approximation to the test data. However, there is a relative large error compared with the test data for the fifth frequency, which we think may be caused by the oversimplification of the vibration isolators during the initial FE

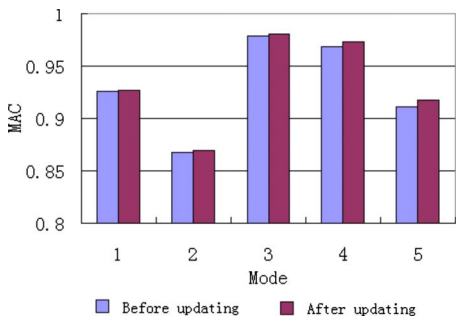

Fig. 11. Change of reduced-test MAC (second updating)

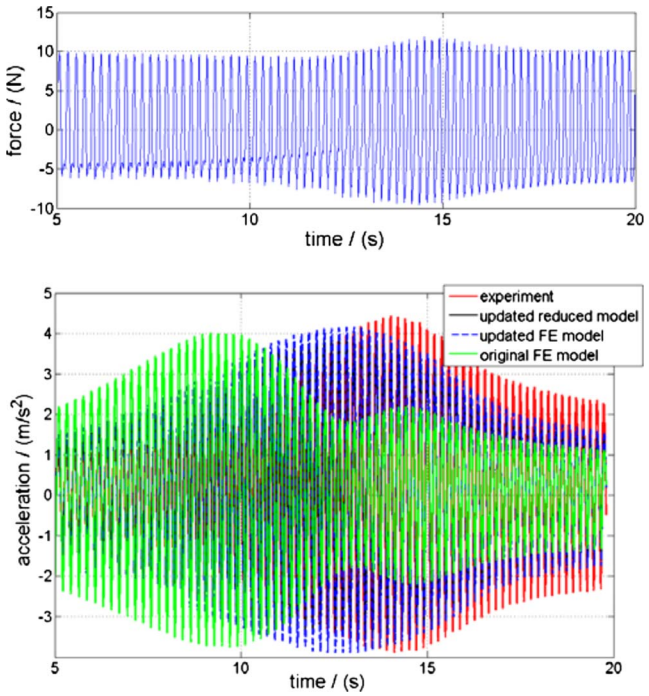

Fig. 12. Response comparison between theoretical predication and experimental data

modeling. The largest relative error is about 2.20% (Fig. 10), still within acceptable precision. To further prove the effectiveness, we draw in time domain the computed acceleration responses of the original FE model, the updated FE model, and the updated reduced model under the same measured force, respectively, and compare them with the measured response at two measuring positions, No. 1 and No. 3 (Fig. 3). Fig. 12 shows an example of damped harmonic response on No. 3 with respect to a sinusoidal frequency-scanning force in y-direction, which is described in Computer-Aided Test section. Because the total signal spans a long range of time, only a period between 5 and 20 s is shown in this window. Its frequency band ranges from about 4.45 to 5.35 Hz, including the first natural frequency. This figure clearly shows that the time when the maximum response happens in the updated analytical models (their response are nearly the same) is much closer to that in the real structure, compared with the original FE model. It indicates that the first natural frequency of the updated models is more consistent with the facts than the original model. Fig. 13 shows another example of damped free vibration under an instantaneous impulse of x-direction. It is obvious that the acceleration response measured in position No. 1 contains two main frequencies, the second and fifth natural frequencies. The computation results have a good consistence with the experiment, except for the original FE model whose response obviously lags behind others after 0.6 s.

Conclusions

The reduction-based model updating method provides an effective way that unites the reduction and updating of a platform structure as one problem. When the reduced model is used for model updating, the computation work can be highly decreased and the difficulty, caused by the incomplete measured data, is greatly mitigated.

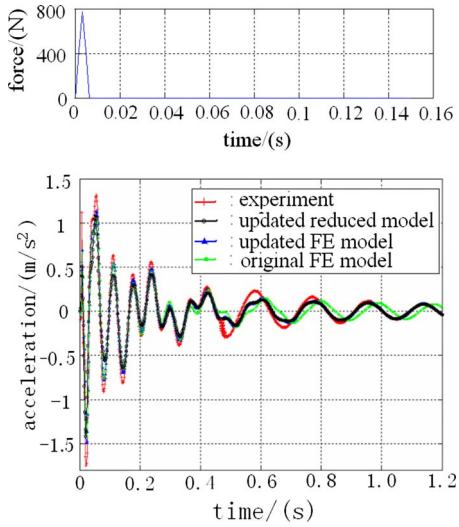

Fig. 13. Response comparison between theoretical predication and experimental data

The reduction method used in the paper makes the reduced model remain the same connecting property as the original FE model, which brings the following updating work at least two advantages. One is that the sensitivity-based parametric method can still be employed without modification. The other is that the method makes model validation possible in that the initial FE model is also calibrated to the real structure at the same time as the reduced model is updated.

Because the proposed reduction method is based on the local-rigidity assumption, it is then restricted to some special structures. The closer the real structure approaches to such assumptions, the better the reduced model, otherwise, an oversimplified or even ill-reduced model may be obtained.

Some difficulties that have not been well cracked in experiment-based model updating were also encountered in the paper, e.g., the selection of structural parameters, which makes an engineer depend on his a priori experience other than the general science. Moreover, a reasonable numerical simulation of real structure is also a key point for a good result of model updating, as shown in the unsatisfied updating result of the higher modes.

Acknowledgments

The work in this paper was supported by the cooperation research project between China National Offshore Oil Corporation (CNOOC) and Chinese Academy of Sciences (Project No. KJCX2-SWL03-01) and also supported by the Knowledge Innovation Program of the Chinese Academy of Sciences. All of the experiments in the paper were completed with the cooperation of Professors Zhonghan Shen and Yubiao Liu in the Institute of Mechanics. Their help is greatly appreciated.

Appendix I. Eigensensitivity Analysis of Reduced Model

Eigensensitivity with respect to Submatrix Scaling Factor

The eigensensitivity of the reduced model with respect to SSF can be calculated using the formula of Fox and Kapoor (1968). Because only stiffness matrix has to be corrected for the reduced model, the derivatives of ith eigenvalue and eigenvector with respect to the jth SSF are simplified as

$$\frac{\partial \omega_i^{\mathrm{R}}}{\partial \alpha_j} = \frac{1}{2\omega_i^{\mathrm{R}}} (\boldsymbol{\varphi}_i^{\mathrm{R}})^{\mathrm{T}} \frac{\partial \mathbf{K}_R}{\partial \alpha_j} \boldsymbol{\varphi}_i^{\mathrm{R}} = \frac{1}{\omega_{R2i}} (\boldsymbol{\varphi}_i^{\mathrm{R}})^{\mathrm{T}} \left(\sum_{r=1}^{q} \alpha_r \boldsymbol{\gamma}_r^{\mathrm{T}} \mathbf{K} \boldsymbol{\gamma}_j \right) \boldsymbol{\varphi}_i^{\mathrm{R}}$$

$$\frac{\partial \boldsymbol{\varphi}_i^{\mathrm{R}}}{\partial \alpha_j} = \sum_{l=1}^{n} \beta_{il} \boldsymbol{\varphi}_l^{\mathrm{R}} \tag{18}$$

$$\left\{ \beta_{il} = \begin{bmatrix} \dfrac{(\boldsymbol{\varphi}_l^{\mathrm{R}})^{\mathrm{T}} \dfrac{\partial \mathbf{K}_R}{\partial \alpha_j} \boldsymbol{\varphi}_i^{\mathrm{R}}}{(\omega_i^{\mathrm{R}})^2 - (\omega_l^{\mathrm{R}})^2} = \dfrac{(\boldsymbol{\varphi}_l^{\mathrm{R}})^{\mathrm{T}} \left(\sum_{r=1}^{q} \alpha_r \boldsymbol{\gamma}_r^{\mathrm{T}} \mathbf{K} \boldsymbol{\gamma}_j \right) \boldsymbol{\varphi}_i^{\mathrm{R}}}{(\omega_i^{\mathrm{R}})^2 - (\omega_l^{\mathrm{R}})^2} & (i \neq l) \\ 0 & (i = l) \end{bmatrix} \right\} \tag{19}$$

Eigensensitivity with respect to Structural Parameters

Similar to Eq. (24), the eigensensitivities can be calculated using the formula of Fox and Kapoor (1968) as

$$\frac{\partial \omega_i^{\mathrm{R}}}{\partial p_j} = \frac{1}{2\omega_i^{\mathrm{R}}} (\boldsymbol{\varphi}_i^{\mathrm{R}})^{\mathrm{T}} \left[\frac{\partial \mathbf{K}_R}{\partial p_j} - (\omega_i^{\mathrm{R}})^2 \frac{\partial \mathbf{M}_R}{\partial p_j} \right] \boldsymbol{\varphi}_i^{\mathrm{R}} \tag{20}$$

$$\frac{\partial \boldsymbol{\varphi}_i^{\mathrm{R}}}{\partial p_j} = \sum_{l=1}^{n} \beta_{il} \boldsymbol{\varphi}_l^{\mathrm{R}}, \quad \left\{ \beta_{il} = \begin{bmatrix} \dfrac{(\boldsymbol{\varphi}_l^{\mathrm{R}})^{\mathrm{T}} \dfrac{\partial \mathbf{K}_R}{\partial p_j} \boldsymbol{\varphi}_i^{\mathrm{R}}}{(\omega_i^{\mathrm{R}})^2 - (\omega_l^{\mathrm{R}})^2} & (i \neq l) \\ -\dfrac{1}{2} (\boldsymbol{\varphi}_i^{\mathrm{R}})^{\mathrm{T}} \dfrac{\partial \mathbf{M}_R}{\partial p_j} \boldsymbol{\varphi}_i^{\mathrm{R}} & (i = l) \end{bmatrix} \right\} \tag{21}$$

where $p_j = j$th structural parameter and $\partial \mathbf{K}_R / \partial p_j$ and $\partial \mathbf{M}_R / \partial p_j$ = derivative matrices of the second reduced stiffness and mass matrices with respect to the parameter p_j. These matrices can be expressed as

$$\frac{\partial \mathbf{K}_R}{\partial p_j} = \boldsymbol{\Gamma}_U^{\mathrm{T}} \frac{\partial \mathbf{K}}{\partial p_j} \boldsymbol{\Gamma}_U \tag{22}$$

and

$$\frac{\partial \mathbf{M}_R}{\partial p_j} = \boldsymbol{\Gamma}^{\mathrm{T}} \frac{\partial \mathbf{M}}{\partial p_j} \boldsymbol{\Gamma} \tag{23}$$

Appendix II. Obtain the Equivalent Experimental Mode Shapes

Generally, experimental mode shapes do not directly describe the rigid-body DOFs of floors so they need to be transformed to the equivalent mode shapes before they can be used in the updating process. According to the local-rigidity assumption, if there are at least two different test points for x-, y-, and z-directions on the ith floor, we can obtain the equivalent mode shape values by calculating the expectation of the measured data on this floor. For the

kth mode and the ith floor, they are expressed as

$$\{\phi_k^R\}_i = \begin{Bmatrix} \phi_k^{Mx} \\ \phi_k^{My} \\ \phi_k^{Mz} \\ \phi_k^{M\alpha} \\ \phi_k^{M\beta} \\ \phi_k^{M\theta} \end{Bmatrix}_i = \begin{Bmatrix} E(\phi_{kj}^x) \\ E(\phi_{kj}^y) \\ E(\phi_{kj}^z) \\ E(\phi_{kj}^z/d_j^y) \\ E(-\phi_{kj}^z/d_j^x) \\ E\left(\frac{\phi_{kj}^y}{d_j^x} - \frac{\phi_{kj}^x}{d_j^y}\right) \end{Bmatrix}_i \quad (j = 1, \ldots, n_i) \tag{24}$$

where subscript k refers to the kth mode; $\{\phi_k^M\}_i = k$th equivalent mode shape vector describing the six rigid-body DOFs of the ith floor; ϕ_{kj}^x, ϕ_{kj}^y, and ϕ_{kj}^z = measured kth mode shape values of the x-, y-, and z-directions for the jth test point on the ith floor; and d_j^x and d_j^y = distances from the jth test point to the mass center of the ith floor in the x- and y-directions, respectively. The denotation $E(\cdot)$ means obtaining the expectation.

References

Ahmadian, H., Gladwell, G. M. L., and Ismail, F. (1997). "Parameter selection strategies in finite element model updating." *ASME J. Vibr. Acoust.*, 119, 37–45.

Arnold, R. R., Citerley, R. L., Chargin, M., and Galant, D. (1985). "Application of Ritz vectors for dynamic analysis of large structures." *Comput. Struct.*, 21(3), 461–467.

Atalla, M. J., and Inman, D. J. (1998). "On model updating using neural networks." *Mech. Syst. Signal Process.*, 12(1), 135–161.

Bampton, M. C. C., and Craig, R. R., Jr. (1968). "Coupling of substructures for dynamic analyses." *AIAA J.*, 6(7), 1313–1319.

Baruch, A. (1984). "Methods of reference basis for identification of linear dynamic structures." *AIAA J.*, 22, 561–563.

Beck, J. L., and Katafygiotis, L. S. (1998). "Updating models and their uncertainties. Part I: Bayesian statistical framework." *J. Eng. Mech.*, 124(4), 455–461.

Benfield, W. A., and Hrude, R. F. (1971). "Vibration analysis of structures by component mode substitution." *AIAA J.*, 9(7), 1255–1261.

Berman, A. (1979). "Mass matrix correction using an incomplete set of measured models." *AIAA J.*, 17, 1147–11748.

Berman, A., and Nagy, E. J. (1983). "Improvement of a large analytical model using test data." *AIAA J.*, 21(8), 1168–1173.

Cha, P. D., and Switkes, J. R. (2002). "Enforcing structural connectivity to update damped systems using frequency response." *AIAA J.*, 40(6), 1197–1203.

Chang, C. C., Chang, T. Y. P., and Xu, Y. G. (2000). "Adaptive neural networks for model updating of structures." *Smart Mater. Struct.*, 9, 59–68.

Chang, C. C., Chang, T. Y. P., and Xu, Y. G. (2002). "Selection of training samples for model updating using neural networks." *J. Sound Vib.*, 249(5), 867–883.

Collins, J. D., Hart, G. C., Hasselman, T. K., and Kennedy, B. (1974). "Statistical identification of structures." *AIAA J.*, 12, 185–190.

Farhat, C., and Hemez, F. M. (1993). "Updating finite element dynamic models using an element-by-element sensitivity methodology." *AIAA J.*, 31(9), 1702–1711.

Fox, R. L., and Kapoor, M. P. (1968). "Rates of change of eigenvalues and eigenvectors." *AIAA J.*, 6(12), 2426–2429.

Friswell, M. I., Garvey, S. D., and Penny, J. E. T. (1995). "Model reduction using dynamic and iterated IRS techniques." *J. Sound Vib.*, 186(2), 311–323.

Friswell, M. I., Garvey, S. D., and Penny, J. E. T. (1998). "The convergence of the iterated IRS method." *J. Sound Vib.*, 211(1), 123–132.

Gladwell, G. M. L., and Ahmadian, H. (1995). "Generic element matrices suitable for finite element model updating." *Mech. Syst. Signal Process.*, 9, 601–614.

Guyan, R. J. (1965). "Reduction of stiffness and mass matrices." *AIAA J.*, 3(2), 380.

Hintz, R. M. (1975). "Analytical methods in component modal synthesis." *AIAA J.*, 13(8), 1007–1016.

Hou, S. N. (1969). "Review of modal synthesis technique and a new approach." *The Shock and Vibration Bulletin*, 40(4), 25–39.

Hurty, W. C. (1965). "Dynamic analysis of structural systems using component modes." *AIAA J.*, 3(4), 678–685.

Imregun, M., Sanliturk, K. Y., and Ewins, D. J. (1995a). "Finite element model updating using frequency response function data—II: Case study on a medium-size finite element model." *Mech. Syst. Signal Process.*, 9(2), 203–213.

Imregun, M., Visser, W. J., and Ewins, D. J. (1995b). "Finite element model updating using frequency response function data—I. Theory and initial investigation." *Mech. Syst. Signal Process.*, 9(2), 187–202.

Jaishi, B., and Ren, W. X. (2005). "Structural finite element model updating using ambient vibration test results." *J. Struct. Eng.*, 131(4), 617–628.

Katafygiotis, L. S., and Beck, J. L. (1998). "Updating models and their uncertainties. Part II: Model identifiability." *J. Eng. Mech.*, 124(4), 463–467.

Katafygiotis, L. S., and Lam, H. F. (2002). "Tangential-projection algorithm for manifold representation in unidentifiable model updating problems." *Earthquake Eng. Struct. Dyn.*, 31, 791–812.

Katafygiotis, L. S., and Yuen, K. V. (2001). "Bayesian spectral density approach for modal updating using ambient data." *Earthquake Eng. Struct. Dyn.*, 30(8), 1103–1123.

Kim, K. O., and Kang, M. K. (2001). "Convergence acceleration of iterative modal reduction methods." *AIAA J.*, 39(1), 134–140.

Kuhar, D. G., and Stahle, C. V. (1974). "A dynamic transformation method for modal synthesis." *AIAA J.*, 12(5).

Lam, H. F., Katafygiotis, L. S., and Mickleborough, N. C. (2004). "Application of a statistical model updating approach on phase I of the IASC-ASCE structural health monitoring benchmark study." *J. Eng. Mech.*, 130(1), 34–48.

Leger, P., and Wilson, E. L. (1987). "Generation of load dependent Ritz transformation vectors in structural dynamics." *Eng. Comput.*, 4(4), 309–318.

Levin, R. I., and Lieven, N. A. J. (1998a). "Dynamic finite element model updating using simulated annealing and genetic algorithms." *Mech. Syst. Signal Process.*, 12(1), 91–120.

Levin, R. I., and Lievin, N A J. (1998b). "Dynamical finite element model updating using neural networks." *J. Sound Vib.*, 210, 593–607.

Levin, R. I., Lievin, N. A. J., and Lowenburg, M. H. (2000). "Measuring and improving neural network generalization for model updating." *J. Sound Vib.*, 238(3), 401–424.

Lim, T. W. (1990). "Submatrix approach to stiffness matrix correction using modal test data." *AIAA J.*, 28(6), 1123–1130.

Lin, R., and Xia, Y. (2003). "A new eigensolution of structures via dynamic condensation." *J. Sound Vib.*, 266, 93–106.

Lin, R. M., Lim, M. K., and Du, H. (1995). "Improved inverse eigensensitivity method for structural analytical model updating." *ASME J. Vibr. Acoust.*, 117, 192–198.

Lu, Y., and Tu, Z. G. (2004). "A two-level neural network approach for dynamic FE model updating including damping." *J. Sound Vib.*, 275, 931–952.

Modak, S. V., Kundra, T. K., and Nakra, B. C. (2002). "Comparative study of model updating methods using simulated experimental data." *Comput. Struct.*, 80, 437–447.

Mottershead, J. E., and Friswell, M. I. (1993). "Model updating in structural dynamics: A survey." *J. Sound Vib.*, 167(2), 347–375.

O'Callahan, J. C. (1989). "A procedure for an improved reduced system (IRS) model." *Proc., 7th Int. Modal Analysis Conf.*, Society for Experiemntal Mechanics, Las Vegas, 17–21.

Pandey, P. C., and Barai, S. V. (1995). "Multilayer perceptron in damage detection of bridge structures." *Comput. Struct.*, 54(4), 597–608.

Paz, M. (1989). "Modified dynamic condensation method." *J. Struct.*

Eng., 115(1), 234–238.
Qu, H. A., and Selvam, P. (2005). "Model order reduction of viscously damped vibration systems using accelerated iterative dynamic condensation." *J. Appl. Mech.*, 72(5), 761–771.
Qu, Z. Q., and Fu, Z. F. (1998). "New structural dynamic condensation method for finite element models." *AIAA J.*, 36(7), 1320–1324.
Rao, G. V. (2002). "Dynamic condensation and synthesis of unsymmetric structural systems." *J. Appl. Mech.*, 69(5), 610–616.
Rubin, S. (1975). "Improved component-mode representation for structural dynamic analysis." *AIAA J.*, 13(8), 995–1006.
Setareh, M., Hanson, R. D., and Peek, R. (1992). "Using component mode synthesis and static shapes for tuning TMDs." *J. Struct. Eng.*, 118(3), 763–782.
Suarez, L. E., and Singh, M. P. (1992a). "Modal synthesis method for general dynamic systems." *J. Eng. Mech.*, 118(7), 1488–1503.
Suarez, L. E., and Singh, M. P. (1992b). "Dynamic condensation method for structural eigenvalue analysis." *AIAA J.*, 30(4), 1046–1054.
Tsuei, Y. G., and Yee, E. K. L. (1989). "Direct component modal synthesis technique for system dynamic analysis." *AIAA J.*, 27(8), 1083–1088.
Wilson, E. L., Yuan, M. W., and Dickens, J. M. (1982). "Dynamic analysis by direct superposition of Ritz vectors." *Earthquake Eng. Struct. Dyn.*, 10, 813–821.
Xia, Y., and Lin, R. (2004). "Improvement on the iterated IRS method for structural eigensolutions." *J. Sound Vib.*, 270, 713–727.
Yuen, K. V., and Katafygiotis, L. S. (2002). "Bayesian modal updating using complete input and incomplete response noisy measurements." *J. Eng. Mech.*, 128(3), 340–350.
Yun, C. B., and Bahng, E. Y. (2000). "Substructural identification using neural networks." *Comput. Struct.*, 77, 41–52.
Zimmerman, D. C., and Widengren, M. (1990). "Correcting finite element models using a symmetric eigenstructure assignment technique." *AIAA J.*, 28(9), 1670–1676.